A Modified Random Phase Approximation of Polyelectrolyte Solutions

A. V. Ermoshkin* and M. Olvera de la Cruz

Department of Materials Science and Engineering, Northwestern University, Evanston, Illinois 60208-3108

Received February 4, 2003; Revised Manuscript Received June 5, 2003

ABSTRACT: We compute the phase diagrams of salt-free polyelectrolyte solutions, using a modified Debye−Hückel approach. We introduce the chain connectivity via the random phase approximation with three modifications. First, we modify the electrostatic potential at short distances to include a boundary on the electrostatic attractions at the distance of closest approach between charges, which is important in semidilute solutions. This modification is shown to act as a hard core contribution in solutions of simple electrolytes. Second, we introduce a cutoff on the integration of the modes of wavelength smaller than the size over which the electrostatic attractions cannot be linearized and strongly perturbed chain are expected. A concentration-dependent cutoff is shown to be essential to predict physically reasonable phase diagrams. Third, ion condensation is included self-consistently. The modification does not give correct phase diagrams without the concentration-dependent cutoff. The combined modifications give phase diagrams in agreement with Monte Carlo simulations.

I. Introduction

Debye−Hückel (DH) theory, derived almost 80 years ago, successfully explains many thermodynamic properties of dilute symmetric electrolyte solutions.[1] Recent computer simulations of hard-sphere ionic fluids[2] show that the DH approach provides a rather accurate estimate of the critical temperature, although it underestimates the critical density. A conceptually simple modification of the DH approach, based on accounting for the interactions of ionic pairs[3] with residual ionic fluid, however, gives better estimates for the critical parameters.[4] This simple addition of nonlinear effects is surprisingly good in ionic fluids. We show here that, in polyelectrolyte solutions, this simple nonlinear ion association (which is referenced as ion condensation) correction, including interactions among associated and nonassociated units, as well as hard-core and finite-size ion effects in the DH approach (which is referenced as the random phase approximation, or RPA) is not enough to predict physically reasonable phase diagrams in polyelectrolytes. We provide here a description of the essential elements that the theory must contain to describe the thermodynamics of polyelectrolyte solutions.

The thermodynamics of linear flexible polyelectrolyte solutions is more complicated than ionic fluids, even under salt-free conditions. The chain conformation is strongly dependent on the distance between charges along their backbone b over the Bjerrum length, l_B:

$$l_B = \frac{e^2}{\epsilon T} \tag{1}$$

Here, e is the unit charge, ϵ the dielectric constant of the media, and T the temperature of the system, in units of the Boltzman constant (k_B). At low l_B/b values, the chains are water-soluble under low ionic conditions. A fraction of counterions are expected to be "condensed"[5] along the chains, to decrease their electrostatic energy. González-Mozuelos and Olvera de la Cruz[6] showed that short-range correlations induced by ion condensation can lead to the monomolecular collapse of strongly charged flexible chains in dilute salt-free solutions. They observed that, although there is no ion condensation at infinite dilution, as soon as the concentration of chains increases to a value above zero, some ions will be around the chains if the value of l_B/b is sufficiently high. These ions change the conformations of the chains.[7] A discontinuous transition from stretched with a renormalized charge to collapsed with zero effective charge as the parameter l_B/b increases and/or as the valence of the counterion increases is predicted.

Many models[8−10] have been proposed to determine the free energy of the dense collapsed conformation. Recent simulations[11] clearly show that the collapsed state is a dense ionic system of highly correlated charges. The transition from stretched to collapsed states in monovalent ions occurs at unphysically large values of l_B/b (the transition can be observed at room-temperature values[10] of l_B/b only in the presence of multivalent ions). A major problem with the existing models of the precipitation is the lack of long-range interactions effects between the chains in the solution.

Recently, a different approach was followed. The possibility of phase transitions that lead to polymer-rich and polymer-poor coexisting phases was analyzed by including only long-range correlations via the RPA in salt-free[12] and salted polyelectrolyte solutions.[13] The RPA, which is widely used to describe polyelectrolyte solutions,[14,15] gives unphysical coexisting curves in the limit of salt-free polyelectrolyte solutions.[12] In particular, the RPA of ideal chains predicts that polyelectrolytes with a l_B/b value of ∼1 are not water-soluble in salt-free solutions with monovalent counterions, which is unphysical. Indeed, the critical temperature increased rapidly as the degree of polymerization (N) increased. Moreover, in the RPA of salt-free solutions, the critical density of monomers decreases as N increases, and it goes to zero as N goes to infinity. The RPA is a linearized theory; therefore, its results are rather unphysical, given that it does not include ion condensation,[5,7,16,17] nor does it include the strong electrostatic

* Author to whom correspondence should be addressed. E-mail: ermosh@onyx.ms.nwu.edu.

10.1021/ma034148p CCC: $25.00
Published on Web 09/11/2003

repulsion between the chains that, in flexible chains, leads to chain stretching in low-ionic-strength solutions.[18,19] Moreover, the RPA predicts a rather fast increase of miscibility as soon as salt is added to the solution.[15] Therefore, the miscibility predicted by RPA in salt-free solutions is not understood; it is not due to short-range correlations induced by condensed ions, nor does it seem to be due to the fluctuations of the free ions.

Recent computer simulations of salt-free linear polyelectrolytes solutions in monovalent counterions have shown that there, indeed, is a two-phase segregation transition that increases as N increases.[20] In contrast to the RPA predicted phase diagrams, however, the simulations reveal a critical density that is rather insensitive to the value of N. Furthermore, the simulations suggest that the critical temperature plateaus rapidly as N increases to a maximum value, which is lower than the value predicted by RPA. A one-component plasma approach to polyelectrolyte solutions gives both a critical density and a critical temperature independent of N.[21] However, the one-component plasma approach ignores the contribution from the fluctuations of the monomers in both the dilute and semidilute branches of the phase diagram. That is, it assumes that the chains provide a constant charge density support over which the counterions fluctuate. The critical temperature in the one-component plasma approach is strongly underestimated in salt-free solutions. At such low effective critical temperatures, the counterions should be strongly bound to the monomers at nonzero chain concentrations.

In this paper, we describe a modified polyelectrolyte RPA model that predicts realistic values of the critical temperature and a critical density that is rather insensitive to N, in agreement with the simulations. The RPA approach described here includes three modifications that make the model applicable in both branches of monomer-poor and monomer-rich concentrations (ρ). The first modification is related to the cutoff in RPA. In salt-free polyelectrolyte solutions, the electrostatic contribution to the free energy of charged Gaussian chains does not reduce to the DH limiting law.[14] Instead, a stronger electrostatic contribution results in salt-free solutions that generate instabilities in the free energy as the monomer concentration goes to zero at room temperature in strongly charged chains.[12] However, scaling arguments[9,22,23] and computer simulations[7,24] show that charged chains are stretched in monovalent ionic solutions on length scales that are smaller and of the order of the inverse screening length (κ^{-1}), which is proportional to a correlation length ξ and an electrostatic persistence length l_p.[25]

Therefore, it is not possible to include the monomer density fluctuations within the RPA, which assumes that the electrostatic interactions are linearized and do not perturb the chain statistics. That is, the RPA breaks down over length scales smaller than ξ (which goes to infinity at infinite dilution in salt-free solutions), because, for these length scales, the potential is strongly nonlinear. On this length scale, the long-range nonlinear electrostatic interactions lead to strongly correlated monomers and counterions, and linearized fluctuations should not be included in the approach.

Here, we introduce a concentration-dependent cutoff proportional to the correlation length ξ in the RPA electrostatic contribution, to include only the contribution from the linear fluctuations. That is, for flexible chains, we include only fluctuation from the unperturbed chains and counterions. We also discuss other possibilities for the cutoff that yield similar modifications in the phase diagram. In particular, we discuss a modification where we assume that the important length scale is the average distance between the ions d ($d \approx \rho^{-1/3}$) rather than the correlation length ξ ($\xi \approx \rho^{-1/2}$). We show that the resulting phase diagrams give values that are similar to the simulations values if and only if the cutoff is concentration-dependent. Modifications of the phase diagrams that involve only the inclusion of ion condensation (see below) do not generate almost N-independent critical concentrations. Moreover, the RPA phase diagram, if we include the fluctuations at length scales shorter than ξ through the use of modified chain statistics (such as rodlike segments) at short length scales, gives also strongly N-dependent critical concentrations. This suggests that fluctuations at short length scales should not be included in the linearized approach.

The second modification in our approach involves including the contribution from the hard core of the ions and the monomers. This modification is important to predict reasonable values for the polymer-rich concentrated branch of the phase diagram. In simple electrolyte solutions, the hard core of the ions is included in the electrostatic contribution to the free energy, to avoid spurious results as the concentration of ions increases. In this paper, we modify the interaction potential and show that our modified potential describes the polyelectrolyte solution at the same level of approximation as the modified DH theory for hard-sphere ionic fluids. Our phase diagrams are similar to those obtained recently via correlation functions.[26]

The third modification is to include ion association self-consistently in the model. Ion association is included here, assuming a strong local electrostatic interaction between the ions and specific sites on the chain. This allows us to include the contribution to the energy from the strongly correlated interactions between ions and monomers. We stress that, in our approach, we do not assume that the condensed ions lead to neutral sites that do not interact with other monomers or the noncondensed ions. A model where neutral noninteracting units are assumed as a result of monovalent ion association gives spurious phase diagrams. That is, at low T or high l_B, when all the ions are condensed, one would find increased miscibility (leading to loops in the phase diagrams), because the neutral pairs do not interact. Instead, our ion association model allows us to include electrostatic interactions among all the charges by including short-range correlation between the condensed ions and the monomers. The degree of ion association is determined self-consistently. We show that, although this modification alone is not enough to predict physically reasonable phase diagrams, it improves the agreement with the computer simulations after it has been added to the aforementioned modifications.

In Section II, we describe the general form of a modified RPA model that includes short- and long-range electrostatic correlations for flexible strongly charged chains in salt-free solutions. In Section III, we discuss the electrostatic interaction potential used in the model and state the problem of the RPA describing charged chains and the required modifications without including

ion association. In Section IV, we include ion association via short-range electrostatic interactions. In Section V, we outline and discuss the results and give some conclusions.

II. Model and Free Energy

Consider a mixture of negatively charged polyelectrolyte chains and a residual ionic fluid. Every chain consists of N monomers, each carrying a charge of $-e$. Every ion carries a charge $+e$. We denote the concentration of monomers as ρ_- and the concentration of ions as ρ_+. Because of electroneutrality, the following condition holds:

$$\rho_- = \rho_+ \tag{2}$$

We write the free energy of the system in the form

$$F = F_{\text{ref}} + F_{\text{el}} \tag{3}$$

Here, F_{ref} is the free energy of the system without any electrostatic interactions and, in the limit of athermal solvents, it can be written as

$$\frac{F_{\text{ref}}}{TV} = \rho_+ \ln \rho_+ + \frac{\rho_-}{N}\ln \rho_- + \frac{1}{a^3}(1-\rho^*)\ln(1-\rho^*) \tag{4}$$

where T and V are the temperature and the volume of the system, respectively. We assume that the monomers of the chains and the ions have the same sizes (a). Therefore, the reduced density ρ^* can be written as

$$\rho^* = a^3\rho \qquad (\text{where } \rho = \rho_+ + \rho_-) \tag{5}$$

The second term on the right-hand side of eq 3 is the electrostatic contribution to the free energy. It consists of two parts:

$$F_{\text{el}} = F_{\text{el}}^{\text{short}} + F_{\text{el}}^{\text{long}} \tag{6}$$

$F_{\text{el}}^{\text{short}}$ takes into account the short-range electrostatic effects (ion condensation); we discuss this term in Section IV. $F_{\text{el}}^{\text{long}}$ accounts for the long-range electrostatics and is given by the RPA approach:[14]

$$\frac{F_{\text{el}}^{\text{long}}}{TV} = \frac{1}{2}\int_\Omega \left[\ln\left(\frac{\det(\hat{g}_k^{-1} + \hat{U}_k)}{\det(\hat{g}_k^{-1})}\right) - Tr(\hat{\rho}\,\hat{U}_k)\right]\frac{d\boldsymbol{k}}{(2\pi)^3} \tag{7}$$

where $\hat{g}_k$ is the matrix of correlation functions between the charges:

$$\hat{g}_k = \begin{pmatrix} g_k^{++} & g_k^{+-} \\ g_k^{-+} & g_k^{--} \end{pmatrix} \qquad (g_k^{+-} = g_k^{-+}) \tag{8}$$

$\hat{U}_k$ is a Fourier image of the matrix of interactions between the charges:

$$\hat{U}_k = \begin{pmatrix} U_k & -U_k \\ -U_k & U_k \end{pmatrix} \tag{9}$$

and $\hat{\rho}$ is the matrix of charge concentrations:

$$\hat{\rho} = \begin{bmatrix} \rho_+ & 0 \\ 0 & \rho_- \end{bmatrix} \tag{10}$$

The integration space of wave vectors k is designated by Ω, as shown in eq 7. The inverse of the matrix $\hat{g}_k$ is given by

$$\hat{g}_k^{-1} = \frac{1}{\det(\hat{g}_k)}\begin{pmatrix} \hat{g}_k^{--} & -\hat{g}_k^{-+} \\ -\hat{g}_k^{+-} & \hat{g}_k^{++} \end{pmatrix} \tag{11}$$

By including this form in eq 7, one obtains

$$\frac{F_{\text{el}}^{\text{long}}}{TV} = \frac{1}{2}\int_\Omega \{\ln[1 + (g_k^{++} + g_k^{--} - 2g_k^{+-})U_k] - (\rho_+ + \rho_-)U_k\}\frac{d\boldsymbol{k}}{(2\pi)^3} \tag{12}$$

In the next section, we neglect any short-range electrostatic effects, assuming that $F_{\text{el}} = F_{\text{el}}^{\text{long}}$. This simplification will help us to explain clearly the form of the potential U_k that we use in eq 12 and help us also to justify the idea of using the finite-size integrational sphere Ω for polyelectrolyte solutions.

III. Electrostatic Free Energy and Phase Diagrams without Ion Association

A. Interactions between Charges. Let us first consider the system of simple electrolytes. For this system, the matrix of correlation functions $\hat{g}_k$ has the following form:

$$\hat{g}_k = \begin{pmatrix} \rho_+ & 0 \\ 0 & \rho_- \end{pmatrix} \tag{13}$$

and the electrostatic free energy can be written as

$$\frac{F_{\text{el}}}{TV} = \frac{1}{2}\int_\Omega (\ln(1+\rho U_k) - \rho U_k)\frac{d\boldsymbol{k}}{(2\pi)^3} \tag{14}$$

For monovalent point charges, the interactions are represented by the Coulomb potential,

$$U^{\text{C}}(r) = \frac{e^2}{r\epsilon} \tag{15}$$

and U_k is readily obtained:

$$U_k = \frac{1}{T}\int U^{\text{C}}(r)\exp(i\boldsymbol{k}\boldsymbol{r})\,d\boldsymbol{r} = \frac{4\pi l_{\text{B}}}{k^2} \tag{16}$$

where l_{B} is given by eq 1. Substituting U_k into eq 14 and integrating over the entire $\boldsymbol{k}$-space, one can obtain

$$\frac{F_{\text{el}}^{\text{C}}}{TV} = -\frac{\kappa^3}{12\pi} \tag{17}$$

where the inverse screening length (κ) is defined as

$$\kappa^2 = 4\pi l_B \rho \tag{18}$$

One can see that eq 17 is the limiting case ($\kappa a \ll 1$) of

the DH expression for the free energy of hard-sphere ionic fluid:

$$\frac{F_{\mathrm{el}}^{\mathrm{DH}}}{TV} = -\frac{\kappa^3}{12\pi}\tau^{\mathrm{DH}}(\kappa a) \tag{19}$$

with

$$\tau^{\mathrm{DH}}(x) = \frac{3}{x^3}\left(\ln(1+x) - x + \frac{x^2}{2}\right) \tag{20}$$

Clearly, the Coulomb potential $U^{\mathrm{C}}(r)$ given by eq 15 cannot be used to describe the system of charges of finite size a if $\kappa a \approx 1$. As the value of κa increases, the hard-sphere interactions between the charges become more and more important and they should be taken into account. For this purpose, we introduce the following form of $U(r)$:

$$U(r) = U^{\mathrm{C}}(r)\left(1 - \exp\left(-\frac{r}{a}\right)\right) \tag{21}$$

which suppresses electrostatic interactions on the scale of the size of the monomer. The Fourier transform of the aforementioned potential can be easily calculated:

$$U_k = \frac{4\pi l_{\mathrm{B}}}{k^2(1 + k^2a^2)} \tag{22}$$

and for the electrostatic free energy, given by eq 14, we get

$$\frac{F_{\mathrm{el}}}{TV} = -\frac{\kappa^3}{12\pi}\tau(\kappa a) \tag{23}$$

where

$$\tau(x) = \frac{1}{x^3}\left(-1 + \frac{3x^2}{2} + \frac{1 + x - 2x^2}{(1+2x)^{1/2}}\right) \tag{24}$$

Another possible way to account for the hard-sphere nature of the charges is to use the Coulomb potential (eq 15) but perform integration in eq 14 within the sphere $\Omega = \Omega_a$, where

$$\Omega_a = \frac{4\pi}{3a^3} \tag{25}$$

This results in the following form of the free energy:

$$\frac{F_{\mathrm{el}}^{\Omega_a}}{TV} = -\frac{\kappa^3}{12\pi}\tau^{\Omega_a}(\kappa a) \tag{26}$$

where

$$\tau^{\Omega_a}(x) = \frac{1}{\pi}\left(2\arctan(x^{-1}) - \frac{\ln(1+x^2) - x^2}{x^3}\right) \tag{27}$$

In Figure 1, we compare the results for $\tau^{\mathrm{DH}}(x)$, $\tau(x)$, and $\tau^{\Omega_a}(x)$, which are given by eqs 20, 24, and 27, respectively. The curves in the figure show similar behavior as the parameter $x = \kappa a$ increases. The figure also shows the phase diagrams in terms of the reduced concentration ρ^*, which is given by eq 5, and the reduced temperature T^*, which is given by

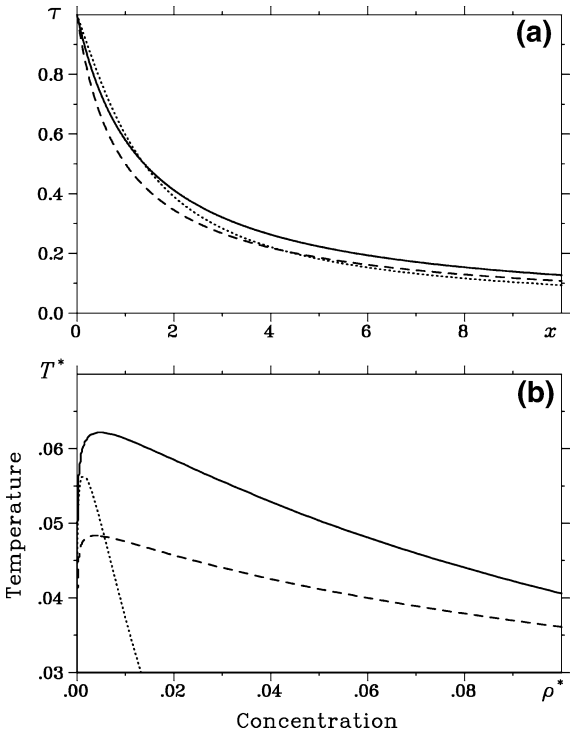

Figure 1. (a) Plots for $\tau(x)$ and (b) the corresponding phase diagrams obtained using eq 19 (solid line), eq 23 (dashed line), and eq 26 (dotted line).

$$T^* = \frac{a}{l_{\mathrm{B}}} \tag{28}$$

The diagrams are obtained using the three different electrostatic free energies, given by eqs 19, 23, and 26. The figure shows that the phase diagram obtained using eq 23 is in reasonable agreement with the DH theory. On the other hand, the phase diagram obtained using eq 26 differs significantly from the DH theory. These results lead us to the conclusion that the hard-core interactions between the charges can be correctly taken into account through the potential $U(r)$ given by eq 21. Moreover, by introducing only a large k cut-off integration parameter in the RPA free energy by eq 25, we cannot recover phase diagrams similar to those obtained using the DH theory. In the next section, we show that a different form of the integrational space Ω should be used to obtain the proper description of *polyelectrolyte* solutions.

B. Wave Vectors and Integrational Space. Let us proceed with the discussion about the integrational space Ω, considering the system of polyelectrolyte chains. Neglecting ion condensation, we write the matrix of correlation functions $\hat{g}_k$ in the form

$$\hat{g}_k = \begin{pmatrix} \rho_+ & 0 \\ 0 & \rho_- g_k \end{pmatrix} \tag{29}$$

where g_k is the structure function of one polyelectrolyte chain and it has the following definition:

$$g_k = \frac{1}{N}\sum_{i,j}\langle \exp[-i\boldsymbol{k}(\boldsymbol{r}_i - \boldsymbol{r}_j)]\rangle \tag{30}$$

Indices i and j in eq 30 run over all monomers of the

chain and the average $\langle ... \rangle$ is taken over all possible chain conformations. The integral (eq 12) now takes the form

$$\frac{F_{el}}{TV} = \frac{1}{2}\int_{\Omega}\{\ln[1 + (\rho_+ + \rho_- g_k)U_k] - \rho U_k\}\frac{d\boldsymbol{k}}{(2\pi)^3} \quad (31)$$

We first examine the dilute case of infinitely long polyelectrolyte chains. To calculate the integral (eq 31) analytically, we will assume that macromolecules obey the Gaussian statistics. For Gaussian chains, the structure factor g_k defined by eq 30 can be approximated as

$$g_k \simeq 1 + \frac{N}{1 + Nb^2k^2/12} \quad (32)$$

where b^2 is the mean-squared distance between the neighboring monomers of the chain. For simplicity, we assume here that $b = a$. In the limit of long chains, g_k takes the form

$$g_k^{\infty} \simeq 1 + \frac{12}{a^2k^2} \quad (33)$$

We also use U_k in the form (eq 16) that is valid for the dilute case $\kappa a \ll 1$, and we rewrite eq 31 in the form

$$\frac{F_{el}}{TV} = \frac{1}{2}\int_{\Omega}\left[\ln\left(1 + \frac{\kappa^2}{k^2} + \frac{6\kappa^2}{a^2k^4}\right) - \frac{\kappa^2}{k^2}\right]\frac{d\boldsymbol{k}}{(2\pi)^3} \quad (34)$$

Evaluation of the aforementioned integral over the entire $\boldsymbol{k}$-space leads to

$$\frac{F_{el}}{TV} = \frac{\kappa^{3/2}}{12\pi a^{3/2}}\tau(\kappa a) \quad (35)$$

where

$$\tau(x) = \frac{12 - \sqrt{6}x - x^2}{(\sqrt{24} + x)^{1/2}} \quad (36)$$

The result $F_{el} \approx \kappa^{3/2}$ for infinitely long Gaussian chains was previously obtained in several papers (see refs 12, 14, and 27).

With the use of eq 35, we take the second derivative of the free energy (eq 3), with respect to the density ρ ($\rho = \rho_+ + \rho_-$), and in the limit of $\rho \to 0$, we find

$$\frac{\partial^2}{\partial\rho^2}\left(\frac{F_{el}}{TV}\right) \simeq \frac{1}{2\rho} - \frac{\kappa^{3/2}}{64\pi b^{3/2}\rho^2} < 0 \quad (37)$$

The negative sign of the second derivative of the free energy shows that dilute solutions of infinitely long polyelectrolyte chains are unstable under good solvent conditions.[12] Figure 2a shows phase diagrams obtained for different chain lengths N. To include the N dependence, we use eq 32 in the electrostatic free energy. The electrostatic contribution to the free energy used to obtain the diagrams is given by

$$\frac{F_{el}}{TV} = \frac{1}{4\pi^2}\int_0^{\infty}\left(\ln\left\{1 + \frac{\kappa^2[1 + 6N/(12 + Nk^2a^2)]}{k^2(1 + k^2a^2)}\right\} - \frac{\kappa^2}{k^2(1 + k^2a^2)}\right)k^2\,dk \quad (38)$$

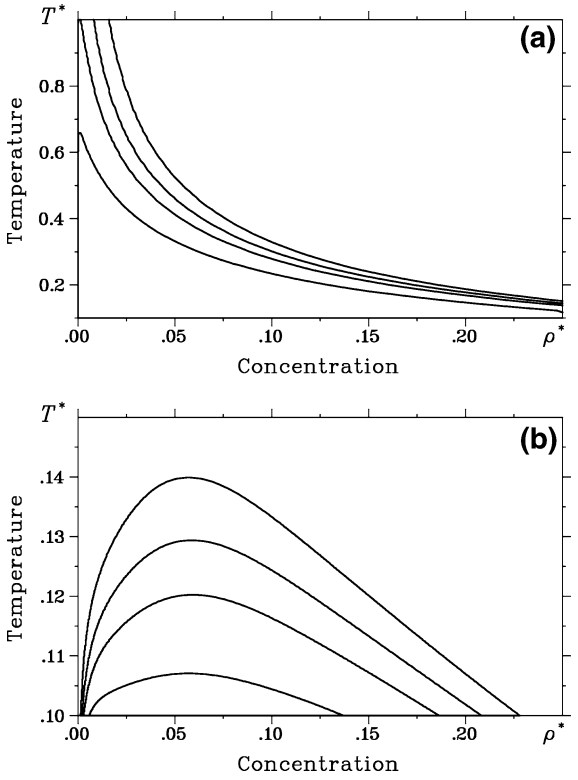

Figure 2. Binodals of salt-free polyelectrolyte solutions obtained within (a) the classical RPA approach and (b) the modified RPA approach for different lengths of the polymers N, in which the condensation of ions onto polymer chains is not taken into account. On each graph, from the lower curve to the upper curve, $N = 25$, 50, 100, and 1000.

and it was evaluated numerically. The figure clearly demonstrates that, as N increases, the region of instability grows and the system becomes unstable, even at very dilute concentrations. The same results will be obtained if the integration is performed over the finite space of $\boldsymbol{k}$-vectors given by eq 25.

The nonphysical behavior described previously results from the inappropriate contribution to the RPA electrostatic free energy at large k. The electrostatic interactions are strong and cannot be linearized at large k, because it is evident in the stretching of the chains due to electrostatics at short length scales. The RPA is only valid if the interactions can be linearized; therefore, the cutoff must be chosen such that we only include the electrostatic contributions that can be determined using the RPA. Determination of the magnitude of the cutoff is straightforward, given that the major feature of polyelectrolyte solutions is the existence of a concentration-dependent correlation length ξ.[22] On the scales smaller than ξ, the chain is stretched; on larger scales, the magnitude of the cutoff obeys Gaussian statistics. For strongly charged polyelectrolytes, ξ can be estimated as[9,23]

$$\xi \approx \frac{1}{(\rho^*)^{1/2}} \quad (39)$$

which is of the order of the inverse screening length. In the Fourier space, scales smaller than ξ are given by $k > 2\pi/(a\xi)$. Because the contributions to the free energy on these scales cannot be determined within the RPA approach, we integrate over $\boldsymbol{k}$ inside the following sphere:

$$\Omega = \frac{4\pi}{3}\mathcal{K}^3 \qquad (\text{where } \mathcal{K} = 2\pi(\rho^*)^{1/2}/a) \qquad (40)$$

Figure 2b shows modified RPA phase diagrams obtained by evaluating the integral (eq 38) up to $k = \mathcal{K}$. The modified RPA phase diagrams have a much lower value of the critical temperature for large N than the standard RPA phase diagrams shown in Figure 2a. The critical temperature T^* initially increases as N increases in the modified RPA phase diagram, and it plateaus at very high N values at $l_B/a \approx 7.1$.

The diagrams presented in Figure 2 demonstrate the importance of the concentration dependence of the large k cutoff given by eq 40. However, the effect of the condensation of ions onto polymer chains is not included in these diagrams. Ion association will not modify the phase diagrams without the cutoff, because, in those systems, the critical temperature is too high to observe significant ion association. However, in the corrected phase diagrams, phase segregation occurs at lower values of T^*, where considerable ion association is expected. In this case, we expect modifications if we include ion association. In the next section, we consider a more realistic system where ion condensation occurs. We show that, indeed, the process of condensation modifies the diagrams given in Figure 2 only quantitatively, supporting the idea about the importance of the integration cutoff that we introduced.

IV. Ion Condensation Effects in the Phase Diagrams

Ion condensation brings two important modifications to the electrostatic free energy of the system previously described by eq 31. First, it gives a nonzero term (F_{el}^{short}, introduced in eq 6); second, it modifies the matrix of correlation functions $\hat{g}_k$ previously given by eq 29.

The term F_{el}^{short} can be written as[28−30]

$$\frac{F_{el}^{short}}{TV} = \rho[\Gamma \ln \Gamma + (1-\Gamma)\ln(1-\Gamma)] - \rho_2 \ln\frac{\rho_2 K}{e} \qquad (41)$$

Here, Γ is the fraction of ions that participate in ion−monomer pair formations, ρ_2 is the concentration of these pairs,

$$\rho_2 = \frac{\rho\Gamma}{2} \qquad (42)$$

and K is the condensation constant, which can be estimated as

$$K \simeq a^3 \exp\left(\frac{l_B}{a}\right) \qquad (43)$$

The first term on the right-hand side of eq 41 corresponds to the number of possibilities from which to choose the monomers and the ions that participate in the formation of pairs, and the second term corresponds to the free energy of all pairs.

Next, we proceed with the evaluation of the matrix of correlation functions $\hat{g}_k$. First, we assume that the condensed ions are distributed randomly along the chain. Second, we suggest that the correlations between the charges of one pair are Gaussian and the average distance between these charges is a. As a result, we consider the system of random copolymer chains that consist of monomers of two types, as illustrated in Figure 3. The correlation functions in this system can be readily calculated.[31]

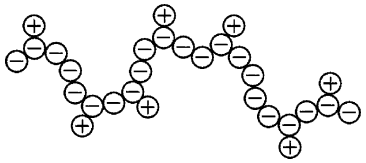

Figure 3. Example of a polyelectrolyte chain with randomly condensed ions.

Let us label the monomers of a particular chain by the index s and introduce the function θ_s such that $\theta_s = 1$ if there is an ion condensed on a monomer s and $\theta_s = 0$ otherwise. Because ions are randomly condensed along the chain, the averages of θ_s have the following properties:

$$\langle\theta_s\rangle = \Gamma \qquad (44)$$

$$\langle\theta_s\theta_{s'}\rangle = \Gamma^2 + \Gamma(1-\Gamma)\delta_{ss'} \qquad (45)$$

Now, the correlation function g_k^{++} can be written as

$$g_k^{++} = \rho_+(1-\Gamma) + \frac{\rho_-}{N}\sum_{s,s'}\exp\left(-\frac{k^2a^2\nu_{ss'}}{6}\right)\langle\theta_s\theta_{s'}\rangle \qquad (46)$$

where

$$\nu_{ss'} = |s-s'| + 2(1-\delta_{ss'}) \qquad (47)$$

The first term on the right-hand side of eq 46 corresponds to the self-scattering of noncondensed ions, the factor ρ_-/N is the concentration of the chains, and the sum gives the average ion−ion correlation within one chain. Taking into account eq 45, one obtains

$$g_k^{++} = \rho_+[1 + \tilde{\Gamma}^2(g_k - 1)] \qquad (48)$$

where g_k is the structure factor of the Gaussian chain, which is approximated by eq 32, and $\tilde{\Gamma}$ is defined as

$$\tilde{\Gamma} = \Gamma\exp\left(-\frac{k^2a^2}{6}\right) \qquad (49)$$

Similarly, for g_k^{+-}, we write

$$g_k^{+-} = \frac{\rho_-}{N}\sum_{s,s'}\exp\left[-\frac{k^2a^2}{6}(|s-s'|+1)\right]\langle\theta_s\rangle \qquad (50)$$

and, with the help of eq 44, one obtains

$$g_k^{+-} = \rho_-\tilde{\Gamma}g_k \qquad (51)$$

The correlations between monomers are not affected by condensation, and they were already described in eq 29.

Substituting expressions obtained for correlation functions into eq 12 for the long-range portion of the electrostatic free energy, one gets

$$\frac{F_{el}^{long}}{TV} = \frac{1}{2}\int_\Omega\left(\ln\left\{1 + \frac{\rho U_k}{2}[1 + (1-\tilde{\Gamma})^2 g_k - \tilde{\Gamma}^2]\right\} - \rho U_k\right)\frac{d\boldsymbol{k}}{(2\pi)^3} \qquad (52)$$

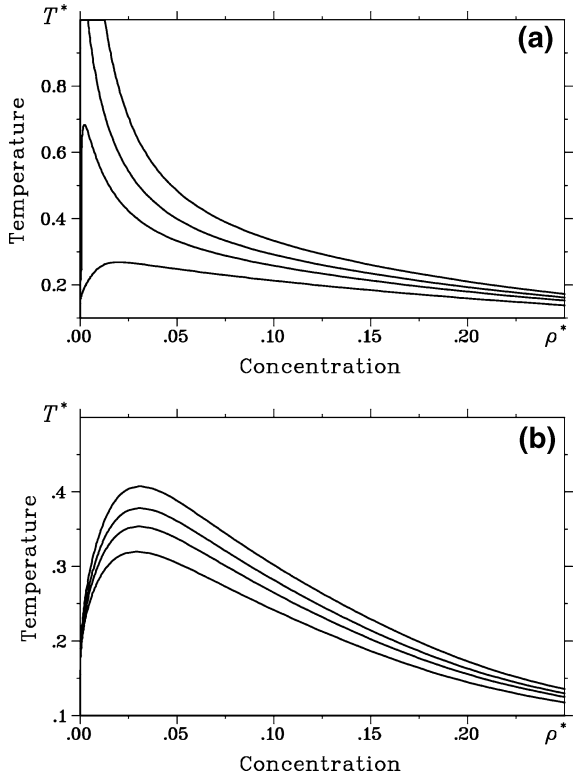

Figure 4. Binodals of salt-free polyelectrolyte solutions obtained within (a) the classical RPA approach and (b) the modified RPA approach for different lengths of the polymers N, in which the condensation of ions onto polymer chains is taken into account. On each graph, from the lower curve to the upper curve, $N = 25$, 50, 100, and 1000.

Figure 4 shows phase diagrams obtained by integrating eq 52 and then minimizing the electrostatic free energy, $F_{el} = F_{el}^{short} + F_{el}^{long}$, with respect to Γ. Figure 4a shows diagrams obtained by integrating eq 52 over the entire $\boldsymbol{k}$-space, and Figure 4b corresponds to the case when integration is performed over the finite sphere Ω, as given by eq 40. The figure clearly shows that ion condensation alone cannot predict physical phase diagrams with water-soluble charged chains unless the concentration-dependent cutoff is taken into account.

V. Results, Discussion, and Conclusions

As follows from Figure 4, salt-free solutions of polyelectrolytes are water-soluble if $l_B/a < 2.5$, which is true for many polymers at room temperature. This critical l_B/a value is obtained using an association constant where the distance of closest approach between monomers is equal to the distance between charges b equal to the ion size. Notice that this value of closest approach is very small in strongly charged chains, suggesting that strongly charged chains with $l_B/b > 2.5$ are not water-soluble in dehydrated monovalent counterions with radii $a < 2.8$ Å. For example, polystyrene sulfonate (PSS) with $l_B/b = 2.8$ may not be water-soluble in ions of sizes $a = b = 2.5$ Å at room temperature. However, in sodium, which is a hydrated ion with $a \simeq 5$ Å, the association constant should be much lower, suggesting that NaPSS is water-soluble, as expected. Comparison of the phase diagrams without ion association, which predict immiscibility for $l_B/a > 7.1$, and the phase diagrams with ion association and a large association constant, which require $l_B/a > 2.5$ for immiscibility, suggests that the RPA phase diagrams are relevant only for very highly charged chains at room temperature.

Another important feature of the modified RPA phase diagrams shown in Figures 2 and 4 is the prediction that the critical concentration remains almost constant as N increases, in agreement with the simulations. This is only true if the contributions from fluctuations of $k > \mathcal{K}$ are completely ignored. That is, if we add the RPA electrostatic contribution from the $1/a > k > \mathcal{K}$ region in the free energy, using the structure function of the strongly perturbed chains (i.e., rodlike), although the critical temperature only increases slightly, the critical concentration goes to zero as N increases. This suggests that the charge fluctuations at lower length scales do not contribute to the free energy or that they are strongly suppressed. The suppression of charge fluctuations on length scales shorter than ξ can be explained by the fact that the electrostatic interactions are not screened at these length scales. Therefore, the counterions and monomers are strongly correlated. Indeed, these correlations stretch the chains.

We have previously argued that, in polyelectrolyte solutions, the cutoff is a natural inverse length scale over which the RPA breaks down. However, it is important to note that a concentration-dependent integration cutoff is also obtained in the one-component plasma,[32] in which counterions fluctuate over a nonfluctuating charged medium. The physical reason for a concentration-dependent cutoff in the one-component plasma explained in ref 32 is different than in polyelectrolytes. Moreover, the form of the concentration-dependent cutoff is very different. In a one-component plasma, the integration in the electrostatic free energy given by the RPA approach should be carried over a finite number of wave-vectors $\boldsymbol{k}$ in the same way as in the Debye theory of the specific heat of solids.[33] Namely, the total number of degrees of freedom in the system, $3\mathcal{N} = 3\rho V$, should be equal to the total number of physically different modes with wave vectors $\boldsymbol{k}$ within the spherical shell $\tilde{\Omega}$. The number of modes is twice the number of wave vectors, because each $\boldsymbol{k}$ has a sine and cosine mode. Therefore, one obtains

$$2V\int_{\tilde{\Omega}} \frac{d\boldsymbol{k}}{(2\pi)^3} = 3\mathcal{N} \tag{53}$$

which leads to

$$\tilde{\Omega} = \frac{4\pi}{3}\tilde{\mathcal{K}}^3 \qquad (\text{where } \tilde{\mathcal{K}} = (9\pi^2\rho)^{1/3}) \tag{54}$$

The aforementioned argument assumes that the important length scale is the average distance between ions ($d \approx 1/\tilde{\kappa} \approx \rho^{-1/3}$), and that this length scales imposes a "periodicity", even though the nonfluctuating support for the ions is a solid with no structure.

The distance between charges ($d \approx \rho^{-1/3}$) is an important length scale to determine the breakdown of the DH theory in simple electrolyte solutions.[8] Therefore, in simple electrolytes, d is an important length scale as the system becomes concentrated. That is, when the electrostatic energy between two charges separated by d is such that $e^2/\epsilon d > k_BT$ or $l_B/d > 1$. Interestingly, the integration to a concentration-dependent cutoff ($\kappa \approx \rho^{1/3}$) versus integration to the inverse hard-core size of the ions ($\kappa \approx 1/a$) does not affect the RPA phase diagrams in simple electrolytes significantly. Instead, in salt-free polyelectrolyte solutions, a concentration-

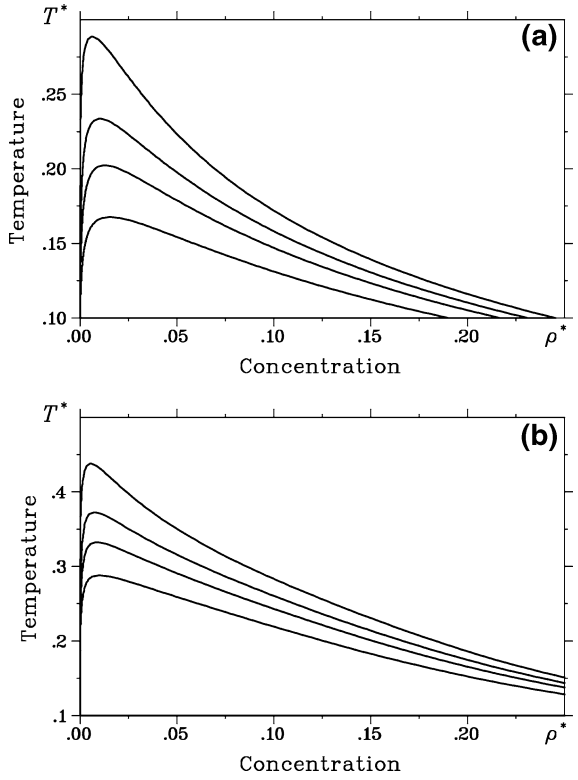

Figure 5. Binodals of salt-free polyelectrolyte solutions obtained within the modified RPA approach with integrational sphere $\tilde{\Omega}$ given by eq 54 (a) neglecting ion condensation and (b) taking ion condensation into account for different lengths of the polymers N. On each graph, from the lower curve to the upper curve, $N = 25$, 50, 100, and 1000.

dependent cutoff is essential to recover reasonable values of the critical temperature as N increases, as well as a critical concentration that is independent of N.

Although we argue that, in salt-free polyelectrolyte solutions, the natural length scale that determines the cutoff is ξ, we obtain very similar phase diagrams if we instead use d, as shown in Figure 5. Notice that the importance of a concentration-dependent cutoff is at dilute solutions where $\xi > d$. Therefore, there should be counterion fluctuations at length scales $d < l < \xi$ that we did not include in our RPA approach. If we add an RPA contribution from these counterion fluctuations (only the counterions), we get negligible corrections to the phase diagram. Our arguments are in agreement with the results in ref 34, where a self-consistent polyelectrolyte RPA shows that, at high wave vectors (short length scales), only counterions contribute to screening. At lower wave vectors, both polyions and counterions contribute to screening. These results are attributed to a polyelectrolyte wave-vector-dependent screening length, because of chain connectivity.

We note that if we include wavelength fluctuations that are shorter than $1/\mathcal{K}$ by modifying the structure function of the chains as rodlike at such wavelengths, we find again unphysical phase diagrams with very small critical concentrations and large critical temperatures as N increases. Furthermore, if we include ion condensation alone (that is, without including a concentration-dependent cutoff), the resulting modified RPA approach gives phase segregation at infinite dilution in large chains. When we include ion association self-consistently and allow for electrostatic interactions among the condensed ions, we obtain reasonable agreement with the simulations only if we include the concentration-dependent cutoff. The concentration cutoff chosen when ion association is included is the same length scale ξ as in the systems without ion condensation. If we, instead, use the actual value of the inverse screening length, which is a function of the degree of ion association, the self-consistent minimization is more complex and will probably lead to negligible corrections to the phase diagrams (we know this because we analyze the effect of different wave-vector-dependent cutoffs in the phase diagrams, such as that used in ref 32). We note that if we did not allow for electrostatic interactions among the condensed ions at low T^*, a window of miscibility appears, because of the fact that all the ions are associated with the chains as $T \rightarrow 0$, resulting in an athermal solution. We do not find this spurious region here, because we found a way to account for the electrostatic interactions among the condensed ions without explicitly including dipole−dipole interactions between the units, as was done in ref 4.

In summary, we show that, in salt-free solutions, a wave-vector-dependent cutoff is essential to recover physical phase diagrams. The cutoff is determined by the applicability limit of the random phase approximation (RPA). In the presence of salt, the electrostatic contribution to the free energy is reduced to the well-known Debye−Hückel (DH) limiting law.[14] In that case, reasonable RPA phase diagrams are obtained without a concentration-dependent cutoff in monovalent salts.[13]

Acknowledgment. We acknowledge the financial support of the National Science Foundation (NSF), through Grant No. DMR-0109610, and A.E. acknowledges partial support from the Nanoscale Science and Engineering Initiative of the NSF, under Award No. EEC-0118025.

References and Notes

(1) Conway, B. E. Ionic Interactions and Activity Behavior of Electrolyte Solutions. In *Comprehensive Treatise of Electrochemistry*; Conway, B. E., Bockris, J. O'M., Yeager, E., Eds.; Plenum Press: New York, 1983; Vol. 5.
(2) Orkoulas, G.; Panagiotopoulos, A. Z. *J. Chem. Phys.* **1999**, *110*, 1581. Yan, Q.; De Pablo, J. J. *J. Chem. Phys.* **1999**, *111*, 9509. Luijten, E.; Panagiotopoulos, A. Z.; Fisher, M. E. *Phys. Rev. Lett.* **2002**, *88*, 045701.
(3) Bjerrum, N. *K. Dan. Vidensk. Selsk.* **1926**, *7*, 9.
(4) Fisher, M. E.; Levin, Y. *Phys. Rev. Lett.* **1993**, *71*, 3826.
(5) Manning, G. S. *J. Phys. Chem.* **1984**, *88*, 6654.
(6) Gonzales-Mozuelos, P.; Olvera de la Cruz, M. *J. Chem. Phys.* **1995**, *103*, 3145.
(7) Stevens, M. J.; Kremer, K. *J. Chem. Phys.* **1995**, *103*, 1669.
(8) Brilliantov, N. V.; Kuznetsov, D. V.; Klein, R. *Phys. Rev. Lett.* **1998**, *81*, 1433.
(9) Schiessel, H.; Pincus, P. *Macromolecules* **1998**, *31*, 7953. Schiessel, H. *Macromolecules* **1999**, *32*, 5673.
(10) Solis, F. J.; Olvera de la Cruz, M. *J. Chem. Phys.* **2000**, *112*, 2030.
(11) Liu, S.; Muthukumar, M. *J. Chem. Phys.* **2002**, *116*, 9975.
(12) Mahdi, K. A.; Olvera de la Cruz, M. *Macromolecules* **2000**, *33*, 7649.
(13) Mahdi, K. A. Ph.D. Thesis, Northwestern University, Evanston, IL, 2000.
(14) Borue, V. Yu.; Erukhimovich, I. Ya. *Macromolecules* **1988**, *21*, 3240.
(15) Joanny, J. F.; Leibler, L. *J. Phys. (Paris)* **1990**, *51*, (6), 545.
(16) Levin, Y. *Rep. Prog. Phys.* **2002**, *65*, 1577.
(17) Netz, R. R.; Andelman, D. *Phys. Rep.* **2003**, *380*, 1.
(18) de Gennes, P. G.; Pincus, P.; Velasco, R. M.; Brochard, F. *J. Phys. (Paris)* **1976**, *37*, 1461.
(19) Barrat, J.-L.; Joanny, J. F. *Europhys. Lett.* **1993**, *24*, 333.
(20) Orkoulas, G.; Kumar Sanat, K.; Panagiotopoulos, A. Z. *Phys. Rev. Lett.* **2003**, *90*, 048303.

(21) Muthukumar, M. *Macromolecules* **2002**, *35*, 9142.
(22) de Gennes, P. G. *Scaling Concepts in Polymer Physics*; Cornell University Press: Ithaca, NY, 1979.
(23) Dobrynin, A. V.; Rubinstein, M. *Macromolecules* **1999**, *32*, 915.
(24) Micka, U.; Holm, C.; Kremer, K. *Langmuir* **1999**, *15*, 4033. Stevens, M.; Kremer, K. *J. Phys. II* **1997**, *6*, 1607.
(25) Liao, Q.; Dobrynin, A. V.; Rubenstein, M. *Macromolecules* **2003**, *36*, 3399.
(26) Jiang, J. W.; Blum, L.; Bernard, O.; Prausnitz, J. M. *Mol. Phys.* **2001**, *99*, 1121.
(27) Olvera de la Cruz, M.; Belloni, L.; Delsanti, M.; Dalbiez, J.; Spalla, O.; Drifford, M. *J. Chem. Phys.* **1995**, *103*, 5781.
(28) Erukhimovich, I. Ya. *J. Exp. Theor. Phys.* **1995**, *81*, 553.
(29) Semenov, A. N.; Rubinstein, M. *Macromolecules* **1998**, *31*, 1373.
(30) Ermoshkin, A. V.; Olvera de la Cruz, M. *Phys. Rev. Lett.* **2003**, *90*, 125504.
(31) Shakhnovich, E. I.; Gutin, A. M. *J. Phys. (Paris)* **1989**, *50*, 1843.
(32) Brilliantov, N. V.; Malinin, V. V.; Netz, R. R. *Eur. Phys. J. D* **2002**, *18*, 339.
(33) Ziman, J. M. *Principles of the Theory of Solids*; Claredon Press: Oxford, U.K., 1964.
(34) Donley, J. P.; Rudnick, J.; Liu, A. J. *Macromolecules* **1997**, *30*, 1188.

MA034148P